Dissociation of CH_3SH^+ by Collisional Activation: Evidence of Nonstatistical Behavior†

P. T. Fenn, Y.-J. Chen, S. Stimson, and C. Y. Ng*

Ames Laboratory, U.S. Department of Energy, and Department of Chemistry, Iowa State University, Ames, Iowa 50011

Received: February 26, 1997; In Final Form: May 13, 1997⊗

We have measured the absolute total cross sections for $CH_2SH^+(CH_3S^+)$, CH_2S^+, HCS^+, HS^+, CH_3^+, and CH_2^+ produced by the collision-induced dissociation (CID) reaction of $CH_3SH^+(1^2A'') + Ar$ in the center-of-mass collision energy range of 1−36 eV. While the onset for CH_3^+ is consistent with the thermochemical threshold for the formation of $CH_3^+ + SH$, the onsets for other product ions are higher than their corresponding thermochemical thresholds. Using a charge transfer probing technique, we conclude that the $m/e = 47$ amu ions observed in the CID reaction have mostly the CH_2SH^+ structure. The relative yields for CH_2SH^+, CH_2S^+, HCS^+, HS^+, CH_3^+, and CH_2^+ formed in the CID reaction, which strongly favor the C−S bond scission process leading to the formation of $CH_3^+ + SH$, are significantly different from those measured in previous photoionization and charge exchange studies. Since the $CH_3^+ + SH$ channel is not among the most stable product channels, this observation suggests that the collision-activated dissociation of CH_3SH^+ is nonstatistical. The high yield for $CH_3^+ + SH$ observed in CID is attributed to the more efficient translational to vibrational energy transfer for the C−S stretch than for the C−H stretches of CH_3SH^+, and to weak couplings between the low-frequency C−S and the high-frequency C−H stretching vibrational modes of CH_3SH^+. The differences in excitation mechanisms for CH_3SH^+ *via* collision activation, photoionization, and charge exchange are responsible for the different fragment ion distributions from CH_3SH^+ observed in these experiments.

I. Introduction

As an important atmospheric pollutant emitted from combustion, industrial, and oceanic sources,[1−8] the photochemistry of methymercapton (CH_3SH) has recently received a great deal of experimental and theoretical attention.[9] Being the simplest alkyl mercapton cation, the structure, energetics, and dissociation dynamics of CH_3SH^+ have also been the focus of many theoretical[10−12] and experimental[13−23] efforts.[24] The dissociation dynamics of CH_3SH^+, which address the fundamental question of hydrogen scrambling, have been investigated previously by charge exchange,[21] mass spectrometry,[13,17,19,20] and photoelectron−photoion coincidence (PEPICO)[22] techniques. In a similar energy range above the ground state of CH_3SH^+, the major product ions observed in the charge exchange and photoionization studies are in agreement, including CH_2SH^+ (CH_3S^+), CH_2S^+, HCS^+, HS^+, and CH_3^+.[19−22]

The *ab initio* potential energy profile for most of the rearrangement and fragmentation reactions involving CH_3SH^+ has been calculated.[11] The dissociation mechanisms are partially rationalized by the isomerization equilibrium between CH_3SH^+ and $CH_2SH_2^+$ prior to fragmentation. The existence of the stable $CH_2SH_2^+$ isomer is also supported by experimental studies.[17] At the time of this calculation[12] and of many previous experimental studies,[13,19−22] the energetics for the CH_3S^+ and CH_2SH^+ isomers were not yet accurately established. Without this energetic information for these isomeric ions, the previous investigations of the dissociation mechanisms for CH_3SH^+ must be considered incomplete.

It is interesting that the breakdown diagrams of CH_3SH^+ obtained in the charge exchange,[21] PEPICO[22] study and estimated in the photoionization mass spectrometric experiment[20] are in qualitative agreement with the prediction[20] of the quasiequilibrium theory (QET). Since CH_3SH^+ in electronic excited states can be formed readily by charge exchange and photoionization processes, the results of the charge exchange and photoionization studies indicate that the couplings between the electronic states and the dissociating degrees of freedom of CH_3SH^+ are good, resulting in efficient energy flow between the internal electronic and vibrational modes of CH_3SH^+.

The energetics (Table 1) and structures for the CH_nS and CH_nS^+ ($n = 1-4$) systems have been accurately determined in recent experimental[9,24−33] and theoretical[10−12] investigations. Motivated by this available information, we have undertaken a study of the $CH_3SH^+ + Ar$ collision-induced dissociation (CID) reaction. The primary goal of this study is to compare the nature of product ions and their relative yields produced in CID, charge exchange,[21] and photoionization.[19,20,22] Collisional activation mainly involves translational to rotational and vibrational energy transfer in the ground potential energy surface of CH_3SH^+. At low collision energies, collisional activation should be equivalent to thermal excitation. Considering that translational to electronic energy transfer is inefficient, it is highly questionable whether collisional activation at low collision energies can access excited electronic states from the ground electronic energy surface of CH_3SH^+. If the region of phase space available to collisional activation is different from that available to charge exchange and photoionization, the branching ratios for the dissociation product channels observed in CID should be different from those formed in the other modes of excitation. In other words, the mechanism for CID of CH_3SH^+ may not be statistical in nature. The comparison of the dissociation product ions observed in CID, charge exchange, and photoionization presented here has revealed fundamental information about the CID mechanism. We have also probed the structure of the $m/e = 47$ amu (mass 47) product ions formed in the CID reaction of $CH_3SH^+ + Ar$ by using the charge exchange probing scheme. The question of hydrogen scrambling[13,17,20,21] during the decomposition of excited CH_3SH^+ has been investigated here by examining the CID reaction of $CH_3SD^+ + Ar$.

† Dedicated to Prof. Yuan T. Lee on the occasion of his 60th Birthday.
⊗ Abstract published in *Advance ACS Abstracts,* July 15, 1997.

S1089-5639(97)00721-4 CCC: $14.00

TABLE 1: Current Recommended Experimental $\Delta_f H°_0$ and IE values for CH_3SH, CH_2SH_2, CH_2SH, CH_3S, CH_2S, CHS, CH_3, CH_2, CH_3SH^+, $CH_2SH_2^+$, CH_2SH^+, $CH3S^+$, CH_2S^+, $HCSH^+$, CHS^+, CSH^+, CH_3^+, and CH_2^+ [a]

species	$\Delta_f H°_0$ (kcal/mol)	IE (eV)
	neutrals	
CH_3SH	-3.0 ± 0.1[b,c]	9.4553 ± 0.0006[d]
CH_2SH_2	61.3[e]	7.48[e]
CH_2SH	37.7 ± 2.0[b]	7.536 ± 0.003[b]
CH_3S	31.4 ± 0.5[f]	9.2649 ± 0.0010[g]
		9.2330 ± 0.0010[g]
CH_2S	28.3 ± 2.0[h]	9.376 ± 0.003[h]
HCS	71.7 ± 2.0[h]	7.412 ± 0.007[h]
H_2S	-4.2 ± 0.2	10.4682 ± 0.0002[i]
HS	34.0 ± 0.6[f]	10.4218 ± 0.0004[j]
CH_3	35.6 ± 0.3	9.8380 ± 0.0004[k]
CH_2	93	10.396 ± 0.003
H	51.63	13.598
	Cations	
CH_3SH^+	215.0 ± 0.1[b,d]	
$CH_2SH_2^+$	221, 233.8	
CH_2SH^+	211.5 ± 2.0[b]	
CH_3S^+	245.0 ± 0.5[f,g]	
CH_2S^+	244.5 ± 2.0[h]	
trans-$HCSH^+$	≈270,[l] 275[e]	
cis-$HCSH^+$	≈270,[l] 277[e]	
HCS^+	243.2 ± 1.9[h]	
CSH^+	314.6[e]	
H_2S^+	237.2 ± 0.2[c,i]	
HS^+	274.3 ± 0.6[f,j]	
CH_3^+	262.5 ± 0.3[c,k]	
CH_2^+	332	

[a] Unless specified, the $\Delta_f H°_0$ and IE values are obtained from ref 30. [b] Reference 27. [c] Reference 30. [d] Reference 23. [e] Gaussian-2 calculations (see ref 12). [f] Reference 25. [g] Reference 26. [h] Reference 28. [i] Reference 31. [j] Reference 32. [k] Reference 33. [l] References 20 and 30.

In the present experiment, the reactant CH_3SH^+ is prepared by photoionization of CH_3SH at its ionization threshold. By using a sufficiently high photon energy resolution, the reactant CH_3SH^+ is formed in its ground vibronic state. Furthermore, since the CH_3SH sample is introduced into the photoionization ion source in the form of a supersonic jet in this experiment, CH_3SH^+ thus formed is also rotationally cold. This is the result of the fact that photoionization only involves small changes in rotational angular momentum. This approach of forming reactant ions by photoionization has many advantages over that by electron impact ionization of a supersonic jet. Due to the lower energy resolution used in electron impact ionization, together with the fact that supersonic expansion is inefficient for vibrational relaxation, reactant ions thus formed may contain considerable vibrational excitations.

On the basis of the self-consistent-field molecular orbital calculation using the 4-31G basis set,[18] the main electronic configuration for CH_3SH is predicted to be

$$...(8a')^2(2a'')^2(9a')^2(10a')^2(3a'')^2$$

The 3a″ orbital is a nonbonding orbital (n_S) localized at the S atom. The 10a′ and 9a′ orbitals are σ-bonding in character and are mainly localized along the C−S (σ_{CS}) and S−H (σ_{HS}) bonds, respectively. The first to fifth photoelectron bands observed in previous He I photoelectron spectroscopic studies[15,16,18] have been assigned to the removal an electron from the 3a″, 10a′, 9a′, 2a″, and 8a′ orbitals, resulting in the $1^2A''$, $1^2A'$, $2^2A'$, $2^2A''$, and $3^2A'$ states for CH_3SH^+. The vertical ionization energies (IEs) for these corresponding states are 9.46, 12.05, 13.73, 15.08, and 15.53 eV.[18] As expected, the vertical and adiabatic IEs for the formation of the ground $CH_3SH^+(1^2A'')$ state are nearly identical due to the similar geometries of CH_3SH and $CH_3SH^+(1^2A'')$.[10] We note that the reactant $CH_3SH^+(1^2A'')$ prepared by photoionization in this experiment has the charge localized mostly at the S atom.

II. Experiment Section

The arrangement of the triple−quadrupole double-octopole (TQDO) photoionization ion−molecule reaction apparatus (Figure 1) and procedures used to perform state-selected absolute total cross-section measurements have been described in detail previously.[34−37] The TQDO apparatus essentially consists of, in sequential order, a vacuum ultraviolet (VUV) photoionization ion source, an electron impact ion source (1), a reactant quadrupole mass spectrometer (QMS) (5), a lower radio frequency (rf) octopole ion guide reaction gas cell (RFOIGGC) [(6) + (7)], a middle QMS (10), an upper RFOIGGC [(11) + (14)], a product QMS (15), and a modified[38] Daly-type scintillation ion detector [(17) + (19) + (20)]. The electron impact ion source is not used in this experiment. The TQDO apparatus is partitioned into five chambers which are separately evacuated by liquid nitrogen- or freon-trapped diffusion pumps.

The photoionization ion source consists of a 0.2 m VUV monochromator (McPherson 234), a hydrogen discharge lamp, and a photoelectric VUV light detector. The recent high-resolution nonresonant two-photon pulsed field ionization photoelectron (N2P-PFI-PE) study of CH_3SH near the ionization threshold yields a value of 9.4553 ± 0.0006 eV (1311 ± 0.08 Å) for the IE of CH_3SH.[23] The N2P-PFI-PE spectrum also reveals a vibrational progression corresponding to excitation of the C−S stretching mode ($\nu_2^+ = 687$ cm^{-1}) of $CH_3SH^+(1^2A'')$.[23,39] Methanethiol is introduced into the photoionization source as a free jet formed by supersonic expansion through a nozzle with a diameter of 75 μm at a stagnation pressure of ≈120 Torr. By setting the photoionization wavelength at 1310 Å and a wavelength resolution of 6 Å [full width at half-maximum (fwhm)], the CH_3SH^+ reactant ions were formed in their ground vibronic states. The rotational temperature of CH_3SH^+ thus formed is expected to be ≤150 K, characteristic of the neutral CH_3SH jet.

For absolute total cross-section measurements, the reactant CH_3SH^+ ions were extracted and guided by the lower QMS (operated at the rf only mode) and the lower rf octopole ion guide to the middle QMS. The middle QMS, functioning as a mass filter, passed only the desired CH_3SH^+ ions to the upper RFOIGGC, where collision-activated dissociation occurred with Ar. The pressure of Ar in the upper RFOIGGC was monitored with an MKS Baratron manometer, and maintained at $2-3 \times 10^{-4}$ Torr. In this pressure range, the CID product ion intensity was found to have a linear dependence on the Ar gas cell pressure. The reactant ions and the product ions formed in the upper RFOIGGC were then mass selected by the product QMS and detected with the modified Daly-type scintillation ion detector.

The reactant ion beam energies were determined by the retarding potential method, using the upper octopole ion guide to retard the reactant CH_3SH^+ ions. The retarding potential curve thus obtained was differentiated to yield the most probable laboratory kinetic energy (E_{lab}) of the reactant ions and the fwhm of the kinetic energy distribution. The E_{lab} resolution for CH_3SH^+ achieved in this experiment was in the range of ±0.2 eV. The collection efficiencies for reactant and product ions were maximized at each center-of-mass collision energy (E_{cm}) by optimizing the dc voltage settings applied to the ion lenses, the octopole ion guides, and the QMSs.

To probe the structure of the mass 47 ions formed in the CID reaction of $CH_3SH^+ + Ar$, we used both the lower and upper RFOIGGCs. Reactant CH_3SH^+ ions prepared by pho-

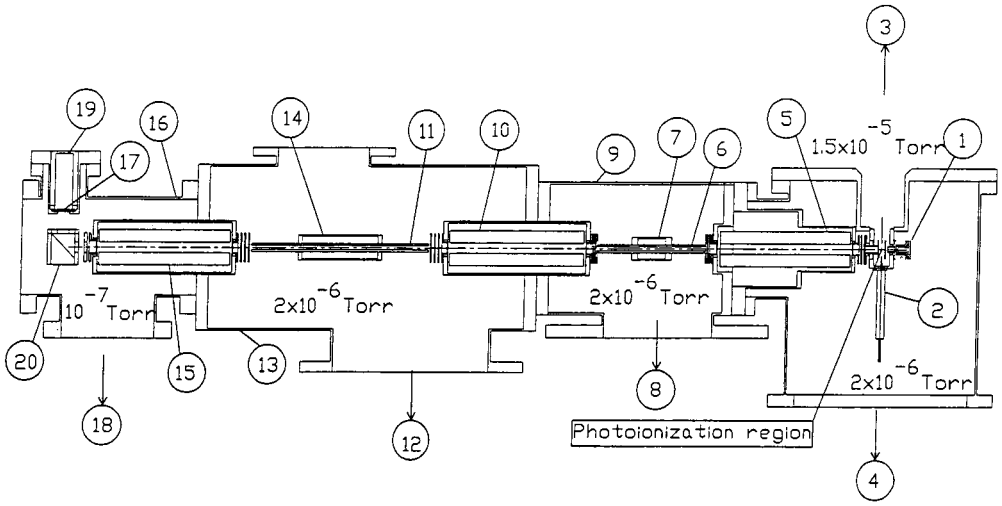

Figure 1. Schematic diagram of the TQDO apparatus: (1) photoionization ion source, (2) atomic or molecular nozzle beam, (3) to freon-trapped 6 in. diffusion pump (DP), (4) to liquid-nitrogen (LN_2)-trapped 6 in. DP, (5) reactant QMS, (6) lower rf octopole ion guide, (7) lower RFOIGGC, (8) to LN_2-trapped 6 in. DP, (9) the lower rf octopole ion guide chamber, (10) middle QMS, (11) upper rf octopole ion guide, (12) to LN_2-trapped 4 in. DP, (13) upper rf octopole ion guide chamber, (14) upper RFOIGGC, (15) product QMS, (16) detector chamber, (17) plastic scintillator window, (18) to LN_2-trapped 2 in. DP, (19) photomultiplier tube, (20) aluminum ion target.

toionization of CH_3SH were first selected by the reactant QMS to enter the lower RFOIGGC, where the CID reaction $CH_3SH^+ + Ar$ took place. The Ar gas cell pressure used was 5×10^{-4} Torr. The mass 47 product ions thus formed in the E_{cm} range of 4.5−6.5 eV were selected by the middle QMS and guided into the upper RFOIGGC, in which the structure for the mass 47 ions was probed by the charge transfer reaction with benzene (C_6H_6) at $E_{cm} \leq 2$ eV. Charge transfer product $C_6H_6^+$ ions, if formed, were detected by the product QMS. The C_6H_6 pressure used in the upper gas cell was 3×10^{-4} Torr. The IEs for CH_3S, CH_2SH, and C_6H_6 are known to be 9.2649 ± 0.0010 eV (ref 26), 7.536 ± 0.003 eV (ref 27), and 9.243 842 ± 0.000 006 eV (ref 40), respectively (see Table 1). Using these IE values, we calculated that the charge transfer reaction (1) for CH_3S^+ is slightly exothermic by 0.0211eV, whereas the charge transfer reaction (2) for CH_2SH^+ is endothermic by more than 1.7 eV. The ΔH°_0 values given in reactions 1 and 2 are the corresponding heats of reaction at 0 K.

$$CH_3S^+ + C_6H_6 \rightarrow CH_3S + C_6H_6^+ \qquad \Delta H^\circ_0 = -0.0211 \text{ eV} \quad (1)$$

$$CH_2SH^+ + C_6H_6 \rightarrow CH_2SH + C_6H_6^+ \qquad \Delta H^\circ_0 = 1.708 \text{ eV} \quad (2)$$

Because near-resonant charge transfer reactions usually have large cross sections, we should observe the formation of $C_6H_6^+$ if the mass 47 ions have the CH_3S^+ structure, while the charge transfer cross section should be negligibly small if CH_2SH^+ ions are produced in the CID reaction of $CH_3SH^+(1^2A'') + Ar$.

It is known that CH_2SH^+ ions are produced at the onset by photoionization of CH_3SH.[19,21,22] This conclusion is based on the fact that the thermochemical threshold of $\Delta H^\circ_0 = 11.541$ eV for process 3 is very close to the appearance energy (AE) of ≈11.55 eV for the mass 47 ion observed in the dissociative photoionization of CH_3SH.

$$CH_3SH + h\nu \rightarrow CH_2SH^+ + H + e^- \qquad \Delta H^\circ_0 = 11.541 \text{ eV} \quad (3)$$

To test the charge transfer detection scheme, we prepared CH_2SH^+ in the photoionization ion source by process 3 at $h\nu$ < 12.4 eV and measured the charge transfer cross section for reaction (2) using the upper RFOIGGC. No $C_6H_6^+$ ions were observed, confirming that CH_2SH^+ is indeed produced by process (3) at $h\nu$ < 12.4 eV. Since the IE(CH_3SH)[23] and IE-(CH_3S)[26] are similar (see Table 1), we have also measured the

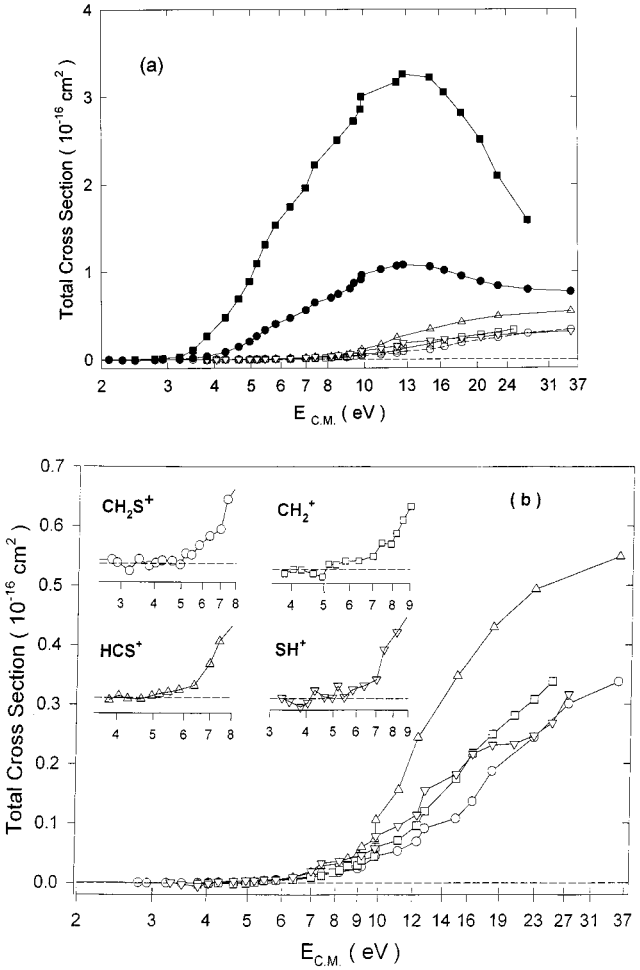

Figure 2. (a) Abolute total cross-section curves for CH_2SH^+ (CH_3S^+) (●), CH_2S^+ (○), HCS^+ (△), HS^+(▽), CH_3^+ (■), and CH_2^+ (□) formed in the CID reaction of $CH_3SH^+ + Ar$ at $E_{cm} = 2-36$ eV. (b) Magnified absolute cross section curves for CH_2S^+(○), HCS^+(△), HS^+(▽), CH_3^+ (■), and CH_2^+ (□).

charge transfer cross section for reaction 4.

$$CH_3SH^+(1^2A'') + C_6H_6 \rightarrow CH_3SH + C_6H_6^+ \qquad \Delta H^\circ_0 = -0.2115 \text{ eV} \quad (4)$$

As expected from the small ΔH°_0 value of -0.2115 eV, we measured a cross section of $\approx$19 Å^2 for reaction (4) at $E_{cm} \approx$ 4−6 eV, yielding a significant intensity of $C_6H_6^+$.

The data acquisition for the TQDO apparatus has recently been upgraded to be controlled by a Pentium PC system.[41] This improvement allows computer control of the QMS and monochromator scans, of the voltage settings applied to individual components of the ion optics system, of the reactant ion kinetic energy determination, and of the background corrections in absolute total cross-section measurements. The procedures outlined above were conducted mostly in an automatic mode.

The methanethiol and benzene were obtained from Aldrich Chemical Co. and Fisher Scientific with purities of 99.5% and 99.9%, respectively. The Ar gas is from Air Products and has a purity of 99.998%.

To examine the aspect concerning H-scrambling in the dissociation of CH_3SH^+, we have also measured the relative intensities of the masses 47 and 48 ions formed in the CID reaction of $CH_3SD^+(1^2A'')$ + Ar. The CH_3SD was obtained from CDN Isotope with a quoted isotopic purity of >91%.

III. Results and Discussion

A. Absolute Total Cross Sections and Identification of CID Product Channels. The product ions observed in the CID reaction of $CH_3SH^+(1^2A'')$ + Ar are CH_2SH^+ (CH_3S^+), CH_2S^+, CHS^+, HS^+, CH_3^+, and CH_2^+. The absolute total cross sections for these product ions in the E_{cm} range of 1.9−37 eV are plotted in Figure 2a. Figure 3 depicts the mass spectrum observed for the CID reaction of CH_3SH^+ + Ar at E_{cm} = 7.3 eV by scanning the product quadrupole mass spectrometer, showing that CH_3^+ and CH_2SH^+ (CH_3S^+) are the major product ions. The cross-section curves for CH_3^+ and CH_2SH^+ (CH_3S^+) have a similar E_{cm} dependence and exhibit a maximum at E_{cm} = 11−14 eV. The maxmium cross section for CH_3^+ is 3.4 Å^2, which is approximately 3 times higher than the maximum cross section of 1.2 Å^2 for CH_2SH^+ (CH_3S^+). A magnified view of the cross section curves for the minor product ions, all of which have cross sections ≤0.5 Å^2, are depicted in Figure 2b. The profiles for the cross section curves of these minor product ions are also similar, *i.e.*, they increase very slowly from their onsets as E_{cm} is increased.

The CID reactions which may be responsible for the production of the observed product ions are given below.

$$CH_3SH^+ + Ar \rightarrow CH_2SH^+ + H + Ar \qquad \Delta H^\circ_0 = 2.09 \pm 0.09 \text{ eV} \quad (5)$$

$$\rightarrow CH_3S^+ + H + Ar \qquad \Delta H^\circ_0 = 3.54 \pm 0.09 \text{ eV} \quad (6)$$

$$\rightarrow CH_2S^+ + H_2 + Ar \qquad \Delta H^\circ_0 = 1.28 \pm 0.09 \text{ eV} \quad (7a)$$

$$\rightarrow CH_2S^+ + H + H + Ar \qquad \Delta H^\circ_0 = 5.75 \pm 0.09 \text{ eV} \quad (7b)$$

$$\rightarrow CHS^+ + H_2 + H + Ar \qquad \Delta H^\circ_0 = 3.46 \pm 0.08 \text{ eV} \quad (8)$$

$$\rightarrow HS^+ + CH_3 + Ar \qquad \Delta H^\circ_0 = 4.12 \pm 0.03 \text{ eV} \quad (9)$$

$$\rightarrow CH_3^+ + SH + Ar \qquad \Delta H^\circ_0 = 3.53 \pm 0.02 \text{ eV} \quad (10)$$

$$\rightarrow CH_2^+ + H_2S + Ar \qquad \Delta H^\circ_0 = 4.89 \text{ eV} \quad (11a)$$

$$\rightarrow CH_2^+ + HS + H + Ar \qquad \Delta H^\circ_0 = 8.8 \text{ eV} \quad (11b)$$

All atomic and molecular species in reactions 5−11 are assumed to be in their ground states. Using the thermochemical data listed in Table 1, we have calculated the corresponding ΔH°_0 values for these reactions. With the exception of minor differences, the nature of the product ions observed in the present CID study are similar to those in previous photoionization[19,20,22] and charge exchange[21] studies in the same energy range.

One of the most important pieces of information obtained in a low-energy CID study, such as this, is the appearance energies (AEs) of the product ions, from which upper limits of the bond dissociation energies involved can be calculated. Although the energetics for the CH_3SH^+ + Ar reaction are well-known, it is still of interest to compare the observed CID AE [AE(CID)] values for product ions with their corresponding thermochemical thresholds. Such a comparison is helpful for identifying the product ions with specific product channels as listed in reactions 5−11. We have listed in Table 2 the AE(CID) values for CH_2SH^+ (CH_3S^+), CH_2S^+, HCS^+, HS^+, CH_3^+, and CH_2^+ determined by the cross section curves of Figures 2(a) and 2(b). Below these AE(CID) values, the intensities of the corresponding product ions are at the background level. Other than the AE(CID) values for CH_3^+ and CH_2SH^+ (CH_3S^+), the AE(CID) value for a minor product ion is given as an E_{cm} range, covering the uncertainty range of the measurement. We note that these AE(CID) values given in Table 2 represent upper limits for the true thermochemical thresholds of the processes involved. We have also fitted the absolute total cross sections for the CID product ions near their onsets using the semiempirical cross section expression,[42]

$$\sigma = \sigma_0 \frac{(E_{cm} - E_0)^n}{E_{cm}} \quad (12)$$

where σ_0, E_0, and n are adjustable parameters. The E_0 value is the onset or AE of the process involved. The best fit values for these parameters are also listed in Table 2. The fits to the total cross sections for CH_2SH^+(CH_3S^+) and CH_3^+ are the most straight forward and reliable, covering the E_{cm} ranges from their respective onsets to ≈12 eV. The E_0 values for CH_2SH^+ (CH_3S^+) (3.84 eV) and CH_3^+ (3.37 eV) are essentially identical to the respective AE(CID) values of 3.9 and 3.5 eV. The fitting to the cross sections for the other minor product ions is complicated by the very gradual rises of the cross section curves near their onsets. The parameters given in Table 2 provide satisfactory fits to the cross section curves for CH_2S^+, HCS^+, HS^+, and CH_2^+, covering the E_{cm} ranges of 5−10, 6−16, 6−15, and 8−15 eV, respectively. The E_0 values for these minor product ions are mostly higher than, but consistent with their corresponding AE(CID) values. The n values for CH_2SH^+ (CH_3S^+) and CH_3^+ are close to unity, which is consistent with a hard-sphere line-of-centers model for energy transfer.[43,44] The

TABLE 2: Appearance Energies Determined in CID and Photoionization and Parameters [(E_0, σ_0, and n, see eq 12] for the Fittings of the CID Cross Sections for CH2SH$^+$ ($CH3S^+$), CH_2S^+, CHS^+, CH_3^+, and CH_2^+ near Their Onsets

product ions	AE(CID)[a] (eV)	E_0[b] (eV)	σ_0 (Å^2)	n	Δ(PI)[c] (eV)
CH_2SH^+/CH_3S^+	3.9 ± 0.2	3.84	1.00	1.23	2.16[d]
					1.8[e]
					1.9[f]
CH_2S^+	5.0−5.5	4.65	0.02	1.74	1.15[d]
					1.12[e]
					1.34[f]
HCS^+	5.0−5.5	6.36	0.11	1.77	<4.15[d]
HS^+	5.5−6.0	5.85	0.12	1.47	
CH_3^+	3.5 ± 0.2	3.37	2.44	1.28	3.90[d]
CH_2^+	5.0−6.0	6.50	0.08	1.54	

[a] This work. Appearance energy determined in the CID study of $CH_3SH^+(1^2A'') + Ar$. The uncertainties represent the precision of the measurements. The uncertainties for CH_2S^+, HCS^+, HS^+, and CH_2^+ are shown by the energy ranges given in the table. [b] See eq 12. E_0 is the onset or AE of the process involved. [c] Appearance energy AE(PI) determined in photoionization mass spectrometric studies of CH_3SH. $\Delta(PI) = AE(PI) - IE(CH_3SH)$. [d] Reference 20. [e] Reference 22. [f] Reference 19.

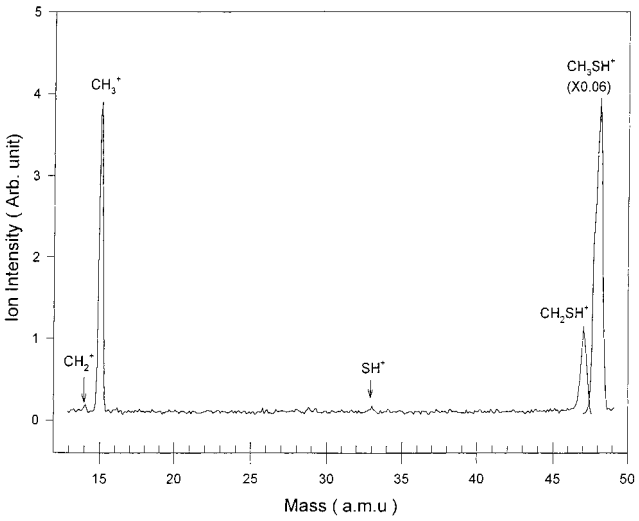

Figure 3. Mass spectrum in the mass range of $m/e = 12-49$ amu for the CID reaction of $CH_3SH^+ + Ar$ obtained at $E_{cm} = 7.3$ eV. The mass peak for $m/e = 48$ amu has been scaled by a factor of 0.06.

n values for other product ions are in the range of 1.5−1.8, which reflect the nonimpulsive character of the collisions at E_{cm}'s near their thresholds.[44]

The AE values for $CH_2SH^+(CH_3S^+)$, CH_2S^+, HCS^+, and CH_3^+ have been reported in previous photoionization studies[19,20,22] of CH_3SH. The photoionization AE [AE(PI)] values represent ionization transition energies with respect to the neutral ground state of CH_3SH. In order to compare these values with the AE(CID) values, it is necessary to subtract the IE(CH_3SH) value (9.4553 ± 0.0006 eV)[23] from the AE(PI) values. Thus, the values for $\Delta(PI) = AE(PI) - IE(CH_3SH)$ given in Table 2 represent the excitation energies measured with respect to CH_3SH^+ in its ground vibronic state. The Δ(PI) values for CH_2SH^+ (CH_3S^+) and CH_2S^+ are in the ranges of 1.8−2.16 eV and 1.12−1.34 eV,[19,20,22] which are in good agreement with the thermochemical thresholds of 2.09 ± 0.09 eV and 1.28 ± 0.09 eV for the formation of $CH_2SH^+ + H$ and $CH_2S^+ + H_2$, respectively, This observation indicates that these product channels are formed in the photoionization experiments at photon energies near the AE(PI)'s of CH_2SH^+ and CH_2S^+. As described in the Experimental Section, no charge transfer product $C_6H_6^+$ was found in the reaction of C_6H_6 with the mass 47 ion formed in the photoionization of CH_3SH. Such an observation is in accord with the conclusion that the mass 47 ions formed by photoionzation have mostly the CH_2SH^+ structure. Although the Δ(PI) values for HCS^+ (<4.15 eV)[20] and CH_3^+ (3.9 eV)[20] are higher by ≈0.5 eV than the respective thermochemical thresholds of 3.46 ± 0.08 eV and 3.53 ± 0.02 eV for the formation of $HCS^+ + H_2 + H$ and $CH_3^+ + SH$, we may still conclude that these product channels are responsible for the production of HCS^+ and CH_3^+ near their photoionization onsets. With the exception of Δ(PI) values for CH_3^+, which is higher than the AE(CID) value for CH_3^+, the Δ(PI) values for CH_2SH^+, CH_2S^+, and HCS^+ are lower than the corresponding AE(CID) values. The AE(PI) values for HS^+ and CH_2^+ were not measured in previous photoionization studies.[19,20,22]

As shown in Figure 2a,b, both the CID onsets for CH_2SH^+ (CH_3S^+) and CH_3^+ are relatively sharp compared to those observed for the other minor product ions, suggesting that CH_3^+, in addition to CH_2SH^+ (CH_3S^+), is formed directly in the CID reaction instead of by secondary decomposition. This conclusion is consistent with the observation that the AE(CID) value of 3.5 ± 0.2 eV for CH_3^+ is in excellent agreement with the thermochemical threshold of $\Delta H°_0 = 3.53 \pm 0.02$ eV for reaction 10. The substantial curvatures and very gradual rises observed for the cross sections of the other minor product ions are mostly indicative of a sequential decomposition or an elimination reaction mechanism involving a tight transition state.

Although the AE(CID) value of 3.9 ± 0.2 eV for the mass 47 ion is higher than the thermochemical threshold of $\Delta H°_0 = 2.09 \pm 0.09$ eV for reaction (5), it is close to that of $\Delta H°_0 = 3.54 \pm 0.09$ eV for reaction (6). It is tempting to speculate that CH_3S^+ is formed near the CID onset for the mass 47 ion. To shed light on the possible structure of the mass 47 ion formed in the CID reaction of $CH_3SH^+ + Ar$, we have carried out a charge transfer probing experiment using the double RFOIGGC scheme as described in the experimental section. On the basis of the energetics of reactions 1 and 2, we expect to observe charge transfer $C_6H_6^+$ if the mass 47 ion has the CH_3S^+ structure, whereas no $C_6H_6^+$ ions should be formed if the mass 47 ion possesses the CH_2SH^+ structure. Since no charge transfer product $C_6H_6^+$ ions are observed, we conclude that the mass 47 ions formed in the CID reaction of $CH_3SH^+(1^2A'') + Ar$ at $E_{cm} = 4.5-6.4$ eV have mostly the CH_2SH^+ structure. This experiment indicates that the closeness between the AE(CID) value for the mass 47 ion and the $\Delta H°_0$ value for reaction (6) is fortuitous.

At the AE(CID) of ≈5.5 eV for HS^+, the product channel should correspond to reaction (9). As pointed out above, the charge of $CH_3SH^+(1^2A'')$ is mainly localized at the S atom. The dissociation of the C−S bond in $CH_3SH^+(1^2A'')$ should result in the formation of $CH_3 + SH^+$. However, during the cleavage of the C−S bond, the charge on HS^+ may hop to CH_3, resulting in the formation of $CH_3^+ + SH$ [reaction 10]. Considering that the IE for CH_3 (9.8380 ± 0.0004 eV)[33] is significantly lower than that of HS (10.4682 ± 0.0002 eV)[32], we expect that the production of $CH_3^+ + SH$ is more favorable than that of $CH_3 + SH^+$, in good accord with the experimental observation.

The AE(CID) value of 5.0−5.5 eV for CH_2S^+ is significantly higher than the thermochemical threshold of $\Delta H°_0 = 1.28 \pm 0.09$ eV for reaction 7a, but lower than the $\Delta H°_0 = 5.75 \pm 0.09$ eV for reaction 7b. Thus, we conclude that $CH_2S^+ + H_2$ are formed at the AE(CID) for CH_2S^+. At $E_{cm} > 5.75$ eV, the formation of $CH_2S^+ + 2H$ is possible. We note that the mass 46 ion can exist as *trans*-$HCSH^+$ and *cis*-$HCSH^+$, which are

estimated to be 1.1 eV higher in energy than CH_2S^+.[12,20,30] We cannot exclude the formation of these structures for the mass 46 ion observed in the CID reaction.

Although the AE(CID) value for HCS^+ determined in the range of 5.0−5.5 eV is higher than the thermochemical threshold of $\Delta H°_0 = 3.46 \pm 0.08$ eV for reaction (8), we may conclude that the formation of HCS^+ is accompanied by H_2 + H at the AE(CID) for HCS^+. The CSH^+ isomer is predicted by Gaussian-2 (G2) *ab initio* calculations to be 3.16 eV higher in energy than that of HCS^+.[12] Thus, the formation of CSH^+ is also possible at higher E_{cm}'s. The formation of $HCS^+ + H_2 +$ H is likely the result of a stepwise dissociation mechanism, *i.e.*, HCS^+ may be produced by the further dissociation of internally excited CH_2SH^+ (CH_3S^+) initially formed by reaction (5) [reaction 6]. Product HCS^+ may also be produced by the decomposition of internally excited CH_2S^+ formed in reaction 7a. However, judging by the significantly higher cross sections for reaction (5) compared to reaction 7a, we favor excited CH_2SH^+ to be the precursor of HCS^+ formed in reaction (8).

The AE(CID) for CH_2^+ is determined to be ≈5.0 eV, which is slightly higher than the thermochemical threshold of $\Delta H°_0 = 4.89$ eV for reactions 11a. This observation indicates that $CH_2^+ + H_2S$ are formed at the CID onset for CH_2^+. Since the IE for CH_2 (10.396 ± 0.003 eV)[30] is only slightly lower than that for H_2S (10.4682 ± 0.0002 eV)[31], it is surprising that H_2S^+ was not observed in the CID reaction. The formation of $CH_2^+ + HS + H$ [reaction 11b] is possible at higher E_{cm}'s. Reaction 11b may result from the further dissociation of excited CH_2SH^+ initially formed by reaction 5 and/or the further dissociation of H_2S formed in reaction 11a.

The aspect concerning H-scrambling in the dissociation of excited CH_3SH^+ has been examined in previous dissociation studies[13,14,20,21] by measuring the relative intensities for product ions from CD_3SH^+. The dissociation product ions observed in these experimental studies indicate that H/D-scrambling may occur before or after the fragmentation processes. We have examined the CID reaction of $CH_3SD^+(1^2A'') + Ar$ at $E_{cm} =$ 10 and 15 eV. Masses 48 and 47 ions are observed with the intensity ratios of ≈ 4:1 and ≈ 2:1 at $E_{cm} = 10$ and 15 eV, respectively, favoring the formation of mass 48. Based on the results of the charge exchange probing experiment, we expect the mass 48 ion to be CH_2SD^+ and the mass 47 ion to be CH_2SH^+. The observed ratios of CH_2SD^+ to CH_2SH^+ are in agreement with the ratios of CD_2SH^+ to CD_2SD^+ from CD_3SH^+ reported in previous mass spectrometric studies.[13,14] The ratio for CH_3^+ to CH_2D^+ from the CID reaction of CH_3SD^+ is also found to decrease from ≈ 4:1 to ≈ 2.5:1 as E_{cm} is increased from 10 to 15 eV. These findings unambiguously show that a finite extent of H/D-scrambling occurs during the collision-activated dissociation of $CH_3SD^+(1^2A'')$.

B. Potential-Energy Profile for Rearrangement and Dissociation Reactions of CH_3SH^+. The *ab initio* potential energy profile for the rearrangement and dissociation reactions of CH_3SH^+ has been calculated at the MP3/6−31G(d,p)//4-31G level of theory.[11,45,46] The calculations indicate that $CH_2SH_2^+$ (methylenesulfonium radical cation) is a stable isomer, which can be formed by a 1,2-hydrogen shift from $CH_3SH^+(1^2A'')$. The existence of $CH_2SH_2^+$ is supported by collisional-activation mass spectrometric experiments.[17] According to the recent G2 *ab initio* calculation,[12] $CH_2SH_2^+$ is a higher energy isomer which lies 0.8 eV above $CH_3SH^+(1^2A'')$. This value is in good agreement with that obtained in Ref. 11. Using the G2 energetic value for $CH_2SH_2^+$, together with the known energetics for the other molecular species involved, we have constructed a potential energy diagram in Figure 4 which shows the rearrangement and dissociation pathways of the CH_3SH^+ system.

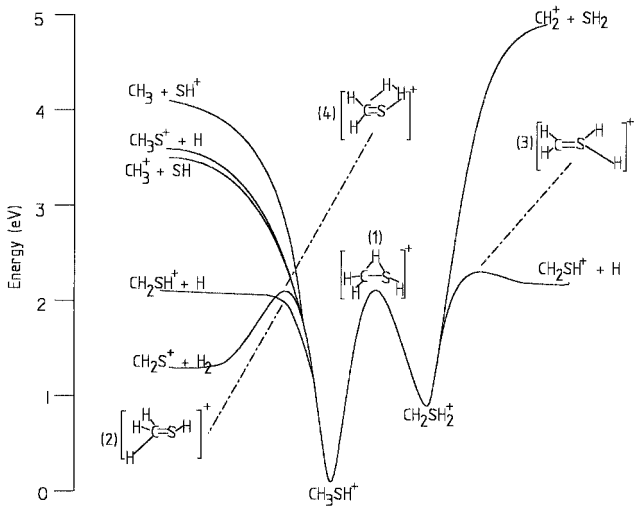

Figure 4. Schematic of the potenial-energy profile for rearrangment and dissociation reactions for CH_3SH^+. For the detailed structures for transition structures **1**, **2**, and **3**, readers are referred to ref 11. See ref 48 for the structure of **4**. The energy for **2** is based on the photoionization AE for CH_2SH^+ (ref 20). The energies for **3** and **4** are based on G2 calculations and that for **1** is from ref 11. The energies for other species are based on thermochemical data of Table 1. See the text.

The transition structure **1** shown in Figure 4 for the 1,2-hydrogen shift between CH_3SH^+ and $CH_2SH_2^+$ is predicted to lie ≈1.97 eV above the energy for $CH_3SH^+(1^2A'')$.[11] Hence, at low excitation energies [<1.97 eV with respect to the energy for $CH_3SH^+(1^2A'')$], these two isomeric ions cannot interconvert. However, the AE(CID) values of all the product ions are above the potential barrier for the 1,2-hydrogen shift. Therefore, both CH_3SH^+ and $CH_2SH_2^+$ should be accessible in this CID experiment. An interesting consequence of the existence of these isomers is that $CH_2SH^+ + H$ can be formed *via* H-eliminations from the C atom of CH_3SH^+ as well as from the S atom of $CH_2SH_2^+$. The corresponding transition structures **2** and **3** for these elimination processes have been calculated to have energies of ≈0.16 eV and ≈0.34 eV above that for $CH_2SH^+ + H$, respectively.[11] We note that the previous *ab initio* calculations predict an energy of ≈1.84 eV[11] for $CH_2SH^+ + H$ with respect to that for $CH_3SH^+(1^2A'')$, which is lower than the known experimental value of 2.09 eV [$\Delta H°_0$ of reaction (5)] by ≈0.25 eV. On the basis of the highest Δ(PI) value of 2.16 eV[20] for CH_2SH^+ (see Table 2), we estimate a potential barrier of ≤ 0.07 eV, as compared to the *ab initio* value of ≈0.16 eV with respect to the energy for $CH_2SH^+ +$ H. The experimental estimate of ≤ 0.07 eV is used to locate the energy of **2** in Figure 4. We have calculated the energies for **2** and **3** at the G2 level of theory.[46−48] The G2 energies for **2** and **3** are found to be 2.10 eV higher than that for CH_3SH^+-$(1^2A'')$, indicating that the reverse potential barrier for the formation of $CH_2SH^+ + H$ from $CH_3SH^+(1^2A'')$ ($CH_2SH_2^+$) is negligibly small. Thus, the G2 prediction is in agreement with the observed AE(PI) values[19,20,22] for CH_2SH^+.

The energy for $CH_3S^+ + H$ is also shown in Figure 4. The ground state for CH_3S^+ is a $^3A_1$ state, which is known to lie 1.45 eV above the ground $CH_2SH^+(^1A')$ state.[10,12] The formation of $CH_3S^+(^3A_1)$ has been demonstrated in photoionization[27,29] and photoelectron[26] experiments. The detailed mechanism for the conversion between $CH_3S^+(^3A_1)$ and $CH_2SH^+(^1A')$ is not known. The rearrangement from $CH_3S^+(^3A_1)$ to CH_2-$SH^+(^1A')$ necessarily involves intersystem crossing from the triplet to the single manifolds, *i.e.*, the coupling between the triplet and singlet potential energy surfaces. The result of the

charge exchange probing experiment, which uses reactions 1 and 2 to probe the existence CH_3S^+, is negative.[49] This observation is consistent with the previous suggestion that the rearrangement from CH_3S^+ to CH_2SH^+ can occur at a sufficiently high internal energy.[17]

As expected, the *ab initio* calculations of ref 11 show that the formations of $CH_3^+ + SH$ from CH_3SH^+ and $CH_2^+ + H_2S$ from $CH_2SH_2^+$ involve loose transition complexes and the reverse activation energies for such processes are zero. Similarly, the formation of $HS^+ + CH_3$ from CH_3SH^+ should also occur without a reverse activation energy. The formation of HCS^+ necessarily involves a two-step dissociation mechanism. Hence, the $HCS^+ + H_2 + H$ channel is not shown in Figure 4.

The Δ(PI) value for CH_2S^+ observed in previous photoionization experiments[19,20,22] are in close agreement with the thermochemical threshold for $CH_2S^+ + H_2$ (see Table 2), indicating that the formation of $CH_2S^+ + H_2$ *via* 1,2-H_2 elimination from CH_3SH^+ may proceed without a reverse potenial energy barrier. The thermochemical threshold (1.28 eV) for the formation of $CH_2S^+ + H_2$ from CH_3SH^+ is lower than the potential energy barrier of 1.97 eV for isomerization from CH_3SH^+ to $CH_2SH_2^+$. Thus, the CH_2S^+ ions observed at the AE for CH_2S^+ in photoionization cannot be formed from $CH_2SH_2^+$. However, the AE(CID) value of 5.0−5.5 observed here is significantly higher than the energy barrier of 1.97 eV for isomerization between CH_3SH^+ and $CH_2SH_2^+$. Hence, the formation of $CH_2S^+ + H_2$ by H_2-elimination from the S atom of $CH_2SH_2^+$ is possible at the AE(CID) of CH_2S^+.

We have obtained the transition structure **4** for 1,2-H_2 elimination from CH_3SH^+ at the MP2/6-311G(d, p) level of theory.[46,50] The G2 energy[48] for (**4**) is found to be 2.08 eV higher than that of CH_3SH^+, which yields a reverse potential energy barrier of 0.8 eV. This prediction is contrary to the photoionization measurements.[19,20,22] A careful examination of the photoionization efficiency spectrum for CH_2S^+ reveals that the yield for CH_2S^+ increased sharply at ≈1075 Å. The photoionization yields below 1075 Å are small. The PEPICO measurement for CH_2S^+ shows negligible yields at photon energies below 1180 Å. Taking this value as the AE for CH_2S^+, we calculate a Δ(PI) value of 2.02 eV for CH_2S^+.[22] Thus, the PEPICO measurement for CH_2S^+ seems to support the G2 prediction. On the basis of the threshold photoelectron spectrum for CH_3SH, the adiabatic IE for the formation of the excited $CH_3SH^+(1^2A')$ is estimated to be ≈1075 Å (11.53 eV) or Δ(PI) ≈ 2.08 eV. The sharp increases in photoionization yields for CH_2S^+, as well as those for CH_2SH^+ at ≈1075−1080 Å, may correlate with the onset of the excited $CH_3SH^+(1^2A')$ state.

As pointed out in ref 11, since the potential energy barriers for the 1,2-hydrogen shift connecting CH_3SH^+ and $CH_2SH_2^+$ and those for H-eliminations from CH_3SH^+ and $CH_2SH_2^+$ to give $CH_2SH^+ + H$ are similar, H/D-scrambling may take place prior to fragmentation. This provides a rationalization for the observation of mixed H/D product ions in the dissociation reactions of CD_3SH^+ and CH_3SD^+.

C. Comparison of Relative Abundances for Product Ions Observed in CID, Charge Exchange, and Photoionization. Figure 5 depicts the plot of the relative abundances in percentages for the observed CID product ions $CH_2SH^+(CH_3S^+)$, CH_2S^+, HCS^+, HS^+, CH_3^+, and CH_2^+. Here, the sum of the abundances for all product ions at a specific E_{cm} is normalized to 100%. As shown in the figure, the relative abundance of CH_3^+ decreases monotonically from 100% to ≈30% as E_{cm} is increased from 3.5 eV to 36 eV. In the same E_{cm} range, the relative abundance of $CH_2SH^+(CH_3S^+)$ remains in the range

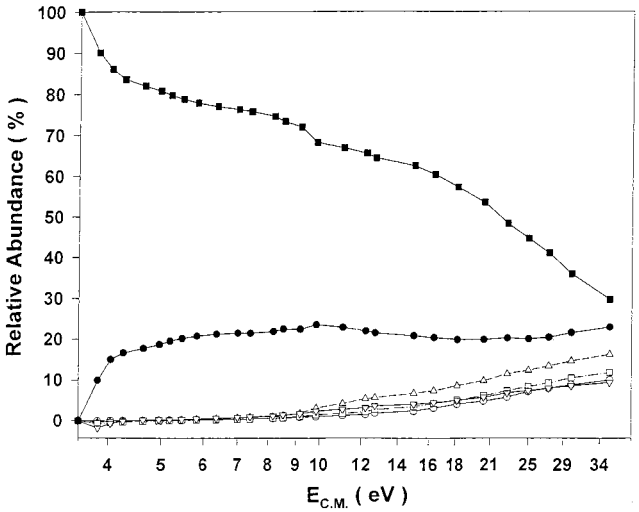

Figure 5. Relative abundances in percentage for CH_2SH^+ (CH_3S^+) (●), CH_2S^+ (○), HCS^+ (△), HS^+(▽), CH_3^+ (■), and CH_2^+ (□) formed in the CID reaction of $CH_3SH^+ + Ar$ at $E_{cm} = 3.5-36$ eV. The sum of all the product ions is arbitrarily set to 100%.

of 15−25%. The relative abundances for other minor product ions are negligibly small at $E_{cm} < 6$ eV and increase gradually as a function of E_{cm} to ≤ 15% at $E_{cm} = 36$ eV.

Table 3 compares the relative abundances for CH_3SH^+, $CH_2SH^+(CH_3S^+)$, CH_2S^+, HCS^+, HS^+, and CH_3^+ observed in this CID experiment with those reported in the previous charge exchange[21] and photoionization mass spectrometric[20] studies in the energy range of 2.7−12 eV. In order to compare the abundances observed in charge exchange and photoionization with those in CID, the recombination energies (RE) of the charge exchange experiment and the photon energies (PHE) in the photoionization experiment are converted to excitation energies (E_{ex}) with respect to the ground vibronic state of $CH_3SH^+(1^2A'')$. That is, the E_{ex} values given in Table 3 are equal to E_{cm} in CID, RE−IE(CH_3SH) in charge exchange, and PHE−IE(CH_3SH) in photoionization. At a specific E_{ex}, the sum of the abundances for all product ions except that for CH_3SH^+ is arbitrarily set to 100%. The abundances of CH_3SH^+ for the CID study are not included in the table because CH_3SH^+ is the reactant ion in this case. Furthermore, since CH_2^+ was not observed in the charge exchange and photoionization studies, the comparison of the abundances for CH_2^+ was also excluded from the table.

Considering that charge exchange favors processes with small energy defects between the reactant and product states, it is essentially a state- or energy-selected technique. However, photoionization mass spectrometry and CID are not. Thus, the comparison in Table 3 among the abundances of product ions observed in CID, charge exchange, and photoionization experiments should be viewed only as qualitative in nature. The small abundances for CH_3SH^+ observed in the charge exchange study is consistent with the expectation that the overwhelming fraction of CH_3SH^+ initially formed are in dissociative excited states, yielding a low intensity for stable CH_3SH^+.

The charge exchange study used Xe^+, CO_2^+, CO^+, Kr^+, N_2^+, Ar^+, and Ne^+ as the charge transfer reactant ions, covering the E_{ex} range of 2.7−12 eV.[21] As shown in Table 3, at $E_{ex} < 4.0$ eV, $CH_2SH^+(CH_3S^+)$ and CH_2S^+ are the only product ions formed in the charge exchange study, with the abundance (98%) for $CH_2SH^+(CH_3S^+)$ significantly greater than that (2%) for CH_2S^+. The lower yield for CH_2S^+ has been rationalized by QET calculations as due to the tight transition state (**4**) involved in the 1,2-H_2 elimination of CH_3SH^+. At $E_{ex} > 4.0$ eV, HCS^+

TABLE 3: Comparison of Relative Abundances in Percentages[a] for CH_3SH^+, CH_2SH^+, CH_3S^+, CH_2S^+, CHS^+, CH_3^+, and CH_2^+ Formed at Excitation Energies $E_{ex} = 2.7-12$ eV[b] in Collisional Activation (CA),[c] Charge Exchange (CE),[d] and Photoionization (PI)[e]

E_{ex} (eV)	exptl	CH_3^+ (15 amu)	HS^+ (33 amu)	HCS^+ (45 amu)	CH_2S^+ (46 amu)	CH_2SH^+ (47 amu)	CH_3SH^+ (48 amu)
2.7	CE	0	0	0	2	98	3
	CA	0	0	0	0	0	
4.0	CE	0	0	0	2	98	3
	CA	85	0	0	0	15	
4−5	CE	2	0	10	6	82	1.5
	CA	81	0	0	0	19	
6−7	CE	3	2	77	8	10	2
	CA	76	1	1	1	21	
	PI	3	1	22	6	68	30
12	CE	3	4	71	10	6	5
	CA	65	3	5	3	22	

[a] The sum of the abundances for all product ions except that for CH_3SH^+ is set to 100%. [b] E_{ex} is the excitation of CH_3SH^+. $E_{ex} = E_{cm}$ in CID, RE − IE(CH_3SH) in charge exchange, and PHE − IE(CH_3SH) in photoionization, where RE and PHE are the recombination and photon energies, respectively. [c] This work. The CID % abundances for CH_3SH^+ are not given in the table because CH_3SH^+ is the reactant ion. At $E_{ex} = 12$ eV, 2% of CH_2^+ is observed in CID. [d] Reference 21. At $E_{ex} = 12$ eV, 2% S^+ and 4% CS^+ are reported in ref 21. [e] Reference 20. At 800 and 744 Å, 0.03% of CH_4 is also observed in ref 20. [e] The structure of the mass 47 ion is expected to be CH_2SH^+. We cannot rule out the formation of CH_3S^+.

and CH_3^+ are also observed in the charge exchange experiment. The abundance for CH_3^+ remains small ≤ 3% in the E_{ex} range of 4−12 eV. Product HS^+, which appears at $E_{ex} >$ 6.0 eV, is also minor, with abundances below 4%. At $E_{ex} =$ 4−12 eV, HCS^+ becomes the dominant product ion. The growth of HCS^+ and CH_2S^+ at higher E_{ex}'s is at the expense of CH_2SH^+. At $E_{ex} = 12$ eV, S^+ and CS^+ with the respective abundances of 2% and 4% are also reported in the charge exchange study.[21]

The relative abundances for fragment ions formed in the photoionization of CH_3SH have been measured at 800 and 744 Å,[20] which are equivalent to $E_{ex} = 6.0$ and 7.2 eV, respectively. In qualitative agreement with the charge exchange study, the abundances for CH_2SH^+ (68%) and HCS^+ (22%) are found to be the dominant product ions. The photoionization mass spectrometric experiment also reported the observation of a small abundance (0.03%) of CH_4^+.

As shown in Table 3, the relative abundances for product ions measured in this CID study reveals CH_3^+ as the major fragment ions with abundances in the range of 65−85% at E_{ex} = 4−12 eV. This abundance is significantly greater than those observed in charge exchange[21] and photoionization studies.[20] Considering that the endothermicities for the formation of $CH_2SH^+ + H$ [reaction (5)], $CH_2S^+ + H_2$ [reaction 7a], and $HCS^+ + H_2 + H$ [reaction 8] are lower than the endothermicity for reaction (10), we expect the abundances for CH_2SH^+, CH_2S^+, and HCS^+ to be greater than that for CH_3^+, as were observed in previous photoionization[19,20,22] and charge exchange[21] experiments. The high abundances for CH_2SH^+, CH_2S^+, and HCS^+ were also predicted by the QET calculations.[20] For a detailed comparison between breakdown diagrams obtained in QET calculations and those derived from the charge exchange and photoionization studies, readers are referred to ref 20.

D. Dissociation Mechanism for Collision Activated CH_3SH^+. The observation that $CH_3^+ + SH$ [reaction (10)] is the dominant product channel over the full E_{cm} range of 2−36 eV is most interesting. Such an observation is contrary to the prediction of QET calculations. The two basic assumptions of a statistical model, such as QET, are that a critical configuration or transition state controls the reaction rate, and that the internal energy of the reactant is randomly distributed in the molecule's active degrees of freedom. This favors the most stable product channel. Hence, the result of the present CID experiment is strong evidence indicating that the CID dissociation of CH_3SH^+ is not compatible with the energy randomization assumption of a statistical model. However, a finite degree of energy flow within CH_3SH^+ clearly takes place, as indicated by the isotopically mixed product ions observed due to H/D-scrambling in the CID measurement of CH_3SD^+.

The statistical model describes, at least qualitatively, the fragmentation resulting from charge exchange and photoionization well, but fails for the fragmentation resulting from collisional activation. The difference between the results of these experiments is in how the necessary internal energy for fragmentation is added to CH_3SH^+. It is known that collisional activation in the E_{cm} range of this experiment is highly inefficient for electronic excitation. A collisional activation process mainly involves translational to rotational and vibrational energy transfer.[43,44] We expect that the low-frequency vibrational modes of CH_3SH^+ are preferentially excited in such a process.[43] The four highest vibrational frequencies[10] of $CH_3SH^+(1^2A'')$ correspond to CH_3 and SH stretching modes, ranging from ≈2556−3035 cm^{-1}, while the C−S stretch[10,39] is the second lowest vibrational mode with a frequency of 687 cm^{-1}. Thus, the internal vibrational energy resulting from collisional activation is predominantly deposited in the C−S stretch mode instead of the CH_3 stretching modes of CH_3SH^+. Furthemore, the fact that S and C are significantly larger than H, may also contribute to the more efficient excitation of the C−S bond in CH_3SH^+. Owing to the large differences in vibrational frequencies between the C−S and CH_3 stretching modes of CH_3SH^+, the C−S and CH_3 stretching modes are only weakly coupled, resulting in inefficient energy flow between the C−S and CH_3 (SH) vibrational modes of CH_3SH^+. As a consequence, the product CH_3^+ ion, which results from the breakage of the C−S bond, is favored over those ions due to the breakage of the C−H (S−H) bonds of CH_3SH^+. This conclusion may be tested in CID studies of larger molecular ions, such as $CH_3CH_2SH^+$, which contains a C−C bond as well as a C−S bond. In addition to the expected efficient excitation of the C−C and C−S stretching modes *via* collisional activation, the coupling between the C−C and C−S modes of $CH_3CH_2SH^+$ should also be good. Hence, product channels arising from the breakage of the C−S and C−C bonds should dominate in the collision activated dissociation of $CH_3CH_2SH^+$.[51]

The observation that the abundances of product ions formed in charge exchange and photoionization are consistent with statistical predictions indicates that the energy randomization assumption is mostly valid when the internal energy of CH_3SH^+ is deposited by electronic excitation. It appears that in the photoionization[20,22] and charge exchange[21] experiments

the onsets of all dissociation product ions are found in the first and second excited photoelectronic bands of CH_3SH^+, *i.e.*, the $CH_3SH^+(1^2A', 2^2A')$ states. As pointed out above, these excited states correspond mainly to the removal of an electron from the σ_{CS} and σ_{HS} bonding orbitals. To a first approximation, the excitations of the C−S and C−H stretching modes of $CH_3SH^+(1^2A')$ and $CH_3SH^+(2^2A')$ are to be expected upon the ejection of an electron from the σ_{CS} and σ_{HS} orbitals of CH_3SH, respectively. Owing to the delocalized nature of these orbitals, such ionization processes are also expected to affect the bonding of the S−H and C−H bonds of CH_3SH^+, resulting in finite excitation of the vibrational modes involving the C−H and S−H bonds. The extent of vibrational excitations in the electronic excited $CH_3SH^+(1^2A', 2^2A')$ states may be assessed by comparing the differences between the equilibrium geometries of the neutral ground CH_3SH state and those of the electronically excited $CH_3SH^+(1^2A', 2^2A')$ states.[23] The more efficient excitation of the low frequency C−S as well as high-frequency CH_3 and S−H vibrational modes of CH_3SH^+ *via* electronic excitations may promote better couplings between these vibrational modes. The Franck−Condon factors for ionization transitions from CH_3SH to the excited $CH_3SH^+(1^2A')$ $CH_3SH^+(2^2A')$ states favor the excitation of a long progression in the C−S and S−H stretching modes, respectively. If several quanta of the C−S stretching mode are excited, the couplings between the C−S and CH_3 (SH) stretching modes should improve.

The CID technique has been used extensively for bond dissociation energy determinations of ionic species.[52] The present study indicates that the CID technique would provide higher sensitivity for the determination of dissociation energies involving bonds of heavy atoms with lower vibrational frequencies. For a dissociation process that proceeds *via* a tight transition state or a stepwise dissociation mechanism, the experimental onset would most likely provide only an upper bound for the dissociation energy for the bond involved.[44]

IV. Conclusions

We have examined the CID reaction of $CH_3SH^+ + Ar$ in the E_{cm} range of 2−36 eV. The fragment ions observed are in general agreement with those observed in previous charge exchange and photoionization studies. The most interesting observation of the present CID study is that $CH_3^+ + SH$ is found to be the dominant product channel, which is contrary to the QET prediction and results of previous charge exchange and photoionization measurements. Stemming from the fact that the dissociation energy for the CH_3^+−SH bond is greater than that of the H−CH_2SH^+ bond, this observation suggests non-statistical behavior in the CID of $CH_3SH^+(1^2A'')$. In effect, this system is an example of bond selective dissociation *via* collisional activation.

The dominant production of $CH_3^+ + HS$ is attributed to the more efficient excitation of the C−S stretch compared to C−H stretches in the collisional activation of CH_3SH^+. The smaller abundances for product ions resulting from C−H bond breakages are rationalized by inefficient intramolecular energy flow due to weak couplings between the C−S and CH_3 stretching modes of $CH_3SH^+(1^2A'')$.

Acknowledgment. This work was supported by the National Science Foundation Grant ATM-9521558. S.S. acknowledges the GAANN Fellowship support for 1994−1995 and 1996−1997.

References and Notes

(1) Benson, S. W. *Chem. Rev.* **1978**, *78*, 23.
(2) Levy, A; Merryman, E. L.; Reid, W. T. *Environ. Sci. Technol.* **1970**, *4*, 653.
(3) Cullis, C. F.; Mulcahy, M. F. R. *Combust. Flame* **1975**, *18*, 225.
(4) Hatakeyama, S; Akimoto, H. *J. Phys. Chem.* **1983**, *87*, 2387.
(5) Turnipseed, A. A.; Barone, S. B.; Ravishankara, A. R. *J. Phys. Chem.* **1993**, *97*, 5926.
(6) Bates, T. S.; Lamb, B. K.; Guenther, A; Dignon, J.; Stroiber R. E. *J. Atmos. Chem.* **1992**, *14*, 315.
(7) Spiro, P. A.; Jacob, D. J.; Logan, J. A. *J. Geophys. Res.* **1992**, *97*, 6023.
(8) Charlson, R. J.; Wigley, T. M. L. *Sci. Am.* **1994**, *270* (2), 48.
(9) Ng, C. Y. *Advances Photochem.* **1997** *22*, 1 and references therein.
(10) Chiu, S.-W.; Li, W.-K.; Tzeng, W.-B.; Ng, C. Y. *J. Chem. Phys.* **1992**, *97*, 6557.
(11) Nobes, R. H.; Bouma, W. J.; Radom, L. *J. Am. Chem. Soc.* **1984**, *106*, 2774.
(12) Curtiss, L. A.; Nobes, R. H.; Pople, J. A.; Radom, L. *J. Chem. Phys.* **1992**, *97*, 6766.
(13) Amos, D.; Gills, R. G.; Occolowitz, J. L.; Pisani, J. F. *Org. Mass Spectrom.* **1969**, *2*, 209.
(14) Keyes B. G.; Harrison, A. G. *J. Am. Chem. Soc.* **1968**, *90*, 5671. Harrison, A. G. *J. Am. Chem. Soc.* **1978**, *100*, 4911.
(15) Frost, D. C.; Herring, F. G.; Katrib, A.; McDowell, C. A.; McLean, R. A. N. *J. Phys. Chem.* **1972**, *76*, 1030.
(16) Cradock, S.; Whiteford, P. A. *J. Chem. Soc., Faraday 2* **1972**, *68*, 281.
(17) Holmes, J. L.; Lossing, F. P.; Terlouw, J. K.; Burgers, P. C. *J. Am. Chem. Soc.* **1982**, *104*, 2931. Terlouw, J. K.; Heerma, W.; Dijkstra, G.; Holmes, J. L.; Burgers, P. C. *Int. J. Mass Spectrom. Ion Phys.* **1983**, *47*, 147. Holmes, J. L.; Lossing, F. P.; Terlouw, J. K.; Burges, P. C. *Can. J. Chem.* **1983**, *61*, 2305.
(18) Kimura, K., Katsumata, S., Achiba, Y., Yamazaki, T., Iwata. S., Eds.; *Handbook of Helium I Photoelectron Spectra of Fundamental Organic Molecules*; Halsted: New York, 1981.
(19) Akopyan, M. E.; Serhiev, Y. L.; Vilesov, F. I. *Klim. Vys. Energy* **1970**, *4*, 305.
(20) Kutina, R. E.; Edwards, A. K.; Berkowitz, J. *J. Chem. Phys.* **1974**, *77*, 5508.
(21) Jonsson, B.-Ö.; Lind,J. *J. Chem. Soc., Faraday Trans. 2* **1974**, *70*, 1399.
(22) Nourbakhsh, S.; Norwood, K.; Yin, H.-M.; Liao, C.-L; Ng, C. Y. *J. Chem. Phys.* **1991**, *95*, 945.
(23) Cheung, Y.-S.; Hsu, C.-W.; Huang, J.-C.; Li, W.-K.; Chiu, S.-W. *Int. J. Mass Spectrom. Ion Processes* **1996**, *159*, 13.
(24) Ng, C. Y. in *The Structure, Energetics, and Dynamics of Organic Ions*; Baer, T., Ng, C. Y., Powis, I., Eds.; Wiley Series in Ion Chemistry and Physics; Wiley: Chichester, 1996; Chapter 2, p 35 and references therein.
(25) Nicovich, J. M.; Kreutter, K. D.; van Dijk, C. A.; Wine, P. H. *J. Phys. Chem.* **1992**, *96*, 2516.
(26) Hsu, C.-W.; Ng, C. Y. *J. Chem. Phys.* **1994**, *101*, 5596.
(27) Ruscic, B; Berkowitz, J. *J. Chem. Phys.* **1992**, *97*, 1818.
(28) Ruscic, B.; Berkowitz, J. *J. Chem. Phys.* **1993**, *98*, 2568.
(29) Nourbakhsh, S.; Norwood, K.; He, G.-Z.; Ng, C. Y. *J. Am. Chem. Soc.* **1991**, *113*, 6311.
(30) Lias, S. G.; Bartmess, J. E.; Holmes, J. L.; Levin, R. D.; Mallard, W. G. *J. Phys. Chem. Ref. Data* **1988**, *17* (Suppl. 1).
(31) Fischer, I.; Lochschmidt, A.; Strobel, A.; Niedner-Schatteburg, G.; Müller-Dethlefs, K.; Bondybey, V. E. *J. Chem. Phys.* **1993**, *98*, 3592.
(32) Hsu, C.-W.; Baldwin, D. P.; Liao, C.-L.; Ng, C. Y. *J. Chem. Phys.* **1994**, *100*, 8047.
(33) Blush, J. A.; Chen, P.; Wiedmann, R. T.; White, M. G. *J. Chem. Phys.* **1993**, *98*, 3557.
(34) Shao, J.-D.; Ng, C. Y. *J. Chem. Phys.* **1986**, *84*, 4317. Shao, J.-D.; Li, Y. G.; Flesch, G. D.; Ng, C. Y. *J. Chem. Phys.* **1987**, *86*, 170. Flesch, G. D.; Ng, C. Y. *J. Chem. Phys.* **1991**, *94*, 2372. Flesch, G. D.; Nourbakhsh, S.; Ng, C. Y. *J. Chem. Phys.* **1990**, *92*, 3490. Flesch, G. D.; Ng, C. Y. *J. Chem. Phys.* **1990**, *92*, 3235.
(35) Ng, C. Y. In *State-Selected and State-to-State Ion-Molecule Reaction Dynamics: I. Experiment*; Ng, C. Y., Baer, M., Eds.; Wiley: New York, 1992. Ng, C. Y. *Adv. Chem. Phys.* **1992**, *82*, 401.
(36) Li, X.; Huang, Y.-L.; Flesch, G. D.; Ng, C. Y. *Rev. Sci. Instrum.* **1994**, *65*, 3724. *Ibid.* **1995**, *66*, 2871.
(37) Li, X; Huang, Y.-L.; Flesch, G. D.; Ng, C. Y. *J. Chem. Phys.* **1997**, *106*, 564.
(38) Gibbs, H. M.; Cummins, E. D. *Rev. Sci. Instrum.* **1966**, *37*, 1385.
(39) The nonresonant two-photon PFI−PE spectrum for CH_3SH obtained in ref 34 also reveals a very small peak at 178 cm^{-1} (0.022 eV) above the IE of CH_3SH, which is assigned as excitation of the ν_1^+ (torsional) mode of $CH_3SH^+(1^2A'')$.
(40) Linder, R.; Müller-Dethlefs, K.; Wedum, E.; Haber, K.; Grant, E. R. *Science* **1996**, *271*, 1698. Chewter, L. A.; Sander, M.; Müller-Dethlefs, K.; Schlag, E. W. *J. Chem. Phys.* **1987**, *86*, 4737. Linder, R.; Sekiya, H.;

Beyl, B.; Müller Dethlefs, K. *Angew Chem., Int. Ed. Engl*. **1993**, *32*, 603. Neuhauser, R. G.; Siglow, K.; Neusser, H. J. *J. Chem. Phys*. **1997**, *106*, 896.

(41) Li, X. *Ph.D. Thesis*, 1996, Iowa State University.

(42) Weber, M. E.; Elkind, J. L.; Armentrout, P. B. *J. Chem. Phys*. **1986**, *84*, 1521.

(43) Mahan, B. H. *J. Chem. Phys*. **1970**, *52*, 5221.

(44) de Sainte Claire, P.; Peslherbe, G. H.; Hase, W. L. *J. Phys. Chem*. **1995**, *99*, 8147. de Sainte Claire, P.; Hase, W. L. *J. Phys. Chem*. **1996**, *100*, 8190.

(45) For CH_4S^+ species, the MP3/6-31G(d, p) energies were estimated by using additivity relationships (see ref 11).

(46) Frisch, M. J.; Trucks, G. W.; Schlegel, H. B.; Gill, P. M. W.; Johnson, B. G.; Robb, M. A.; Cheeseman, J. R.; Keith, T. A.; Petersson, G. A.; Montgomery, J. A.; Raghavachari, K.; Al-Laham, M. A.; Zakrzewski, V. G.; Ortiz, J. V.; Foresman, J. B.; Cioslowski, J.; Stefanov, B. B.; Nanayakkara, A.; Challacombe, M.; Peng, C. Y.; Ayala, P. Y.; Chen, W.; Wong, M. W.; Andres, J. L.; Replogle, E. S.; Gomperts, R.; Martin, R. L.; Fox, D. J.; Binkley, J. S.; Defrees, D. J.; Baker, J.; Stewart, J. P.; Head-Gordon, M.; Gonzalez, C.; Pople, J. A. *Gaussian 94, Revision A.1*; Gaussian, Inc., Pittsburgh, PA, 1995.

(47) Curtiss, L A.; Raghavachari, K.; Trucks, G. W.; Pople, J. A. *J. Chem. Phys*. **1991**, *94*, 7221.

(48) The G2 energies for CH_3SH^+, **2**, **3**, and **4** are −437.800 900, −437.723 698, −437.723 698, and −437.724 606 hartree, respectively. See ref 11 for the structures of **2**, and **3**.

(49) The structure of mass 47 ions formed in the CID of $CH_3SH^+(1^2A")$ at $E_{cm} = 4.5-6.5$ eV are probed in the charge exchange probing experiment. This E_{cm} range corrsponds to the internal excitation energy range of 1−3 eV for $CH_3S^+(^3A_1)$.

(50) The geometric parameters for the MP2/6−311G(d,p) structure of (**4**) are r(CS) = 1.589 Å, r(SH) = 1.477 Å, r[CH(1)] = 3.079 Å, r[CH(2)] = r[CH(3)] = 1.091 Å, ∠CSH = 96.1°, ∠H(1)CS = 55.4°, ∠H(2)CS = 123.6°, ∠H(3)CS = 118.6°, ∠H(1)CSH = ∠H(2)CSH = 0.0°, ∠H(3)CSH = 180.0°, where r's and ∠'s are bond distances and bond angles, respectively. The transition structure is planar, with one of the hydrogen atoms, H(1), originally bound to the C atom stretched to combine with the H atom on the S atom. The S−H bond is increased by 0.12 Å from the equilibrium value in CH_3SH^+.

(51) This expectation has been confirmed in our recent CID study of $CH_3CH_2SH^+ + Ar$. Here, the formation of $CH_3CH_2^+ + SH$ is found to be the dominant channel, followed by $CH_3 + CH_2SH^+$. The lowest energy product channel corresponding to the formation of $CH_3CHSH^+ + H$ was not observed. For more information, see: Chen, Y.-J.; Fenn, P. T.; Stimson, S. *J. Chem. Phys*. In press.

(52) Armentrout, P. B.; Baer, T. *J. Phys. Chem*. **1996**, *100*, 12866.